Effect of Dissolved Glassware on the Structure-Sensitive Part of the Cu(111) Voltammogram in KOH

Tiwari, Aarti; Maagaard, Thomas; Chorkendorff, Ib; Horch, Sebastian

Published in:
ACS Energy Letters

Link to article, DOI:
10.1021/acsenergylett.9b01064

Publication date:
2019

Document Version
Publisher's PDF, also known as Version of record

ACS Energy LETTERS

Cite This: ACS Energy Lett. 2019, 4, 1645−1649

http://pubs.acs.org/journal/aelccp

VIEWPOINT

Effect of Dissolved Glassware on the Structure-Sensitive Part of the Cu(111) Voltammogram in KOH

Electrocatalysis with the aim of converting electrical energy from sustainable sources into synthetic fuels or base chemicals for industrial production has become an important field in research.[1−3] One interesting electrochemical reaction in that context is the direct electrochemical hydrogenation of CO_2 that not only allows storing renewable energy but also helps to close the anthropogenic carbon cycle.[4−9] Since the pioneering work of Hori in the 1980s,[10] Cu remains the only pure metal that can convert CO_2 to higher-value products like higher hydrocarbons and their alcohols in significant amounts. Despite many years of research, the reason for this unique behavior is not yet fully understood, and considerable effort is therefore devoted to elucidate the fundamental electrochemical properties of various Cu-model systems (see Nitopi et al. and references therein[9]).

Whereas there are many results on polycrystalline and amorphous Cu indicating for example that product selectivity and activity are strongly structure dependent,[11] not many results are reported on single-crystalline Cu samples with well-defined facets exposed to the electrolyte that could, for example, elucidate the nature of the active site(s).[12−22] This seems partially due to the fact that Cu is difficult to work with because of its oxophilic nature and partly because the electrochemical (EC) response as measured by cyclic voltammetry (CV) is very sensitive to the exact preparation procedure employed.[23] For example, there is not yet any consensus in the literature about the blank CV scans of low-index Cu single crystals (SCs) in alkaline media, especially in the underpotential region of Cu_2O formation, which is known to be structure-sensitive.[21,23−27] This region can easily drown when investigating CV results of Cu in wide potential windows.[15,28−30]

The fact that the structure-sensitive, intrinsic EC response of low-index Cu facets is not yet unambiguously established hampers the efforts of understanding the special properties of Cu in several ways. First, such blank CV scans are needed as benchmarks for theoretical investigations trying to calculate CV results under more complicated reaction conditions.[31,32] Second, blank CV scans are needed as fingerprints when it comes to establishing whether a model system (e.g., Cu(*hkl*)-oriented films) behaves like a SC electrochemically.[22,33] Third, fingerprint CV scans are needed to analyze polycrystalline samples, where the relative abundance of different facets is deduced by a deconvolution of the measured CV into the CVs of the principal facets.[22,34,35] This again hampers ongoing work on investigating structural changes of polycrystalline Cu or Cu nanoparticles under reaction conditions, where the knowledge of the fundamental CV scans of the various Cu facets is crucial once more.[36]

This Viewpoint provides insight on the observed discrepancies in such fingerprint CV scans. To this end, a combination of scanning tunneling microscopy (STM), EC, inductively coupled plasma mass spectrometry (ICP-MS), and X-ray photoelectron spectroscopy (XPS) was applied in combination with an ultrahigh vacuum (UHV)-EC setup that allows preparation and electrochemical analysis of Cu SCs under very well-controlled conditions.[23] To begin, we compared our CV measurement to the well-known work by Schouten et al.[27] which reported CV results of different low-index Cu surfaces in the underpotential region of Cu_2O formation. This study is widely used as the benchmark for Cu surfaces as evident from subsequent papers.[18−20,22] Surprisingly, we obtained both contrasting and rapidly changing electrochemical results. While searching for possible explanations, we found two studies by Mayrhofer et al.[37,38] about the impact of glass corrosion on the electrocatalytic properties of platinum electrodes in alkaline media, which turned out to be very inspiring for our investigations.

To simplify the story, we restrict ourselves to reporting the results of our extensive analysis of the impact of using glassware on the EC response of one Cu facet, namely Cu(111). Several Cu(111) SCs were investigated under various well-defined conditions in order to eliminate possible sample-, preparation-, or setup-related artifacts. To this end, we investigated SCs in both the above-mentioned dedicated UHV-EC setup and a conventional three-electrode one-compartment EC setup. Both setups consistently show the same influence of glass corrosion on the Cu(111) CV scans in the underpotential region of Cu_2O formation, i.e., the region usually used for benchmarking purposes.

Measurement Details. As samples we used various Cu(111) single crystals (MaTeck, Jülich (DE); purity 99.9999%; typical diameter of the exposed facet 6 mm; thickness 3 mm) which were cleaned and prepared either by sputtering and annealing in the UHV-EC setup or by electropolishing in the case of the conventional setup.

The structure and cleanliness of the UHV-prepared SCs were verified in UHV by STM. Afterward, the SCs were transferred under vacuum to a cube attached to the UHV chamber. The cube was then vented with Ar (6.0, AGA), and an EC cell made of Kel-F was inserted into the cube. EC measurements were carried out under a steady flow of Ar. The electrolyte was a 0.1 M KOH (99.995 Suprapur, Merck) solution made using Millipore water (18.2 MΩcm, Merck Millipore) in volumetric flasks made of either glass (Blau

Received: May 16, 2019
Accepted: June 10, 2019

DOI: 10.1021/acsenergylett.9b01064
ACS Energy Lett. 2019, 4, 1645−1649

Brand) or PFA (Corning Life Sciences). The electrolyte was bubbled with N_2 (5.0, AGA) in a supply bottle made of glass (for electrolyte prepared in a glass flask) or PFA (for electrolyte prepared in a PFA flask) and connected to the EC cell by PFA tubing (IDEX Health & Science). The experimental method and the UHV-EC setup is shown in Figure S1 and described in more detail in a recent publication.[23]

The setup for conventional EC measurements was a PTFE cell (Pine Research) where the working electrode was a Cu SC housed in a PTFE holder compatible with a Pine Research rotator shaft (shown in Figure S2). Before these measurements, the Cu SC was electropolished against a Cu wire in 66% H_3PO_4 (85% EMSURE, Merck) at 2.0 V for 30 s while being rotated at ∼200 rpm. Finally it was rinsed in deaerated Millipore water. The electrolyte was deaerated directly in the cell through a PFA tube (Savillex).

All EC measurements were performed with a Bio-Logic SP200 potentiostat controlled by Bio-Logic's EC-Lab software. A Pt wire was used as the counter and a calibrated RHE as the reference electrode.

Behavior of Cu(111) under Alkaline Conditions. The first measurements were performed on UHV-prepared samples. These were exposed to 0.1 M KOH electrolyte prepared in different ways:

(A) freshly prepared KOH in a PFA flask
(B) freshly prepared KOH in a glass flask
(C) KOH stored overnight in a PFA flask
(D) KOH stored overnight in a glass flask

Apart from the different procedures for electrolyte preparation, the rest of the experiment remained the same for all the measurements. All electrolytes were deaerated and then used to measure the base voltammogram of the clean Cu SC sample in the potential range from −0.20 to +0.45 V vs RHE at a scan rate of 100 mV/s in Ar atmosphere. The samples were immersed in the electrolyte under potential control at 0.33 V vs RHE and then swept cathodically to begin the CV. The results obtained for the different variants of electrolyte are summarized in Figure 1.

As clearly seen, the CV measurments using KOH from a PFA flask irrespective of it being fresh or old show just one relatively sharp and reversible redox feature at 0.11 V vs RHE corresponding to a charge of 76.3 ± 2.4 $\mu C/cm^2$, or 0.27 ± 0.01 electrons per surface atom. Contrastingly, for KOH prepared in glass flasks, we measured different redox features depending on the contact time of KOH with the glass. The KOH freshly prepared in a glass flask traced a similar redox feature as seen for PFA but with additional cathodic reduction waves negative of the main feature. On the other hand, KOH left overnight in a glass flask had a considerably different redox behavior resulting in two oxidative and two reductive peaks with a clear peak separation between the anodic and cathodic scan. This very much resembles CV results previously reported in the literature (cf. Figure S5).

After having established a benchmark CV scan of Cu(111) prepared by sputter/anneal cycles in UHV, we then performed similar measurements on a separate Cu(111) SC prepared by electropolishing in a conventional setup. To do so, we housed the Cu SC in a custom-made PTFE holder that exposes only the crystal face to the electrolyte. The PTFE cell was maintained under Ar atmosphere during EC measurements. After electropolishing, CV scans were recorded using the same

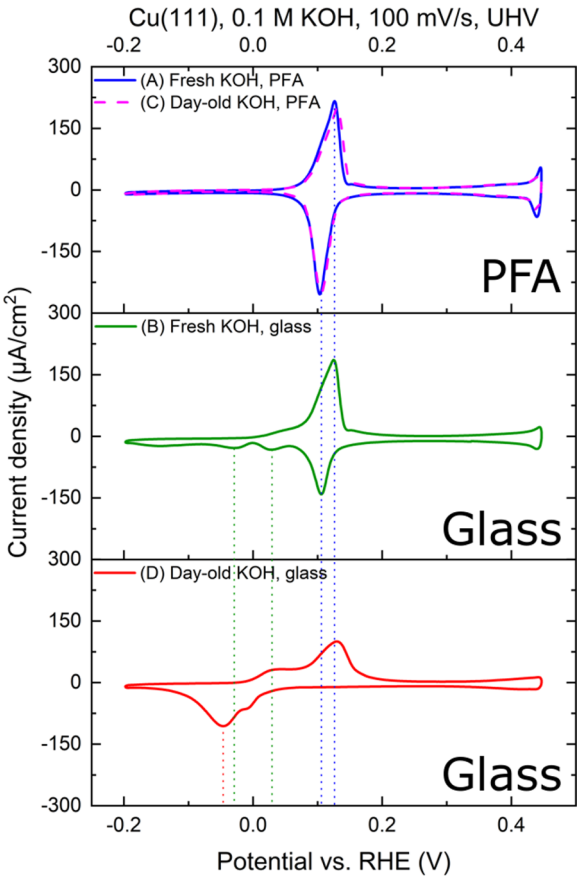

Figure 1. CV scans measured on the UHV-prepared Cu(111) samples in 0.1 M KOH prepared in different ways. The samples were immersed under potential control at 0.33 V vs RHE. CV results from electropolished samples are shown in Figure S3, including a measurement in 0.1 M NaOH.

parameters as in the UHV-EC setup. The CV measurements on the electropolished samples are shown in Figure S3 and compare very well to those in Figure 1. This showed that the features measured on the Cu(111) SC are consistent across both setups and independent of the crystals used, as long as they are well-defined and clean. We note that the reversible feature in the clean case turns out to be composed of two peaks. The dependence of these two peaks on, for example, the exact potential range used is currently under investigation.

To investigate what constituents of the electrolytes might be the reason for the different features seen when using glass and PFA flasks, electrolyte samples were retrieved from the EC cells after CV measurements (shown in Figure 1) for the four cases of electrolyte explored and analyzed using ICP-MS. On the basis of a semiquantitative analysis of a brief survey of all elements, we identified only B, Al, and Si as being present in significant amounts in KOH from a glass flask compared to KOH from PFA; thus, we performed a thorough analysis of these three elements (see the Supporting Information for details). Inspired by Mayrhofer's papers,[37,38] we also checked for Pb but could not detect it in noticeable amounts. The data from this analysis is listed in Table 1 and also shown as a bar graph in Figure 2a. It can clearly be seen that the amounts of these constituents increases significantly with the time that the electrolyte is in contact with glass.

In parallel, we investigated the Cu SC electrode after the EC measurements by transferring the samples to a separate setup

DOI: 10.1021/acsenergylett.9b01064
ACS Energy Lett. 2019, 4, 1645−1649

Table 1. Concentrations of B, Al, Si, and Pb Detected by ICP-MS in the Various Electrolytes[a]

	concentration [ppb]			
electrolyte	B (DL = 0.229)	Al (DL = 0.191)	Si (DL = 8.927)	Pb (DL = 0.002)
(A) fresh KOH, PFA	<DL	1.0	<DL	<DL
(B) fresh KOH, glass	2.1	7.7	61.9	<DL
(C) day-old KOH, PFA	<DL	0.6	8.3	<DL
(D) day-old KOH, glass	264.8	135.1	3450.8	0.01

[a]The detection limit (DL) is noted as well. The same data is shown in Figure 2a.

and performing XPS. Among the different samples we performed XPS on those exposed to electrolyte C and D, as these were exposed to the highest concentrations of impurities. Figure 2b shows a comparative survey spectrum for a clean Cu(111) SC prior to exposure to electrolyte and after EC cycling for 100 cycles in the two electrolytes (C and D), respectively. The main Cu peaks are consistent across all the samples, but on both the Cu SCs which have seen electrolyte, additional peaks are found for K 2p, O 1s, and C 1s. These could be attributed to the electrolyte and adventitious carbon from the atmosphere during sample transfer from the EC-cell into the XPS chamber. Surprisingly we did not observe any of the contaminants seen from ICP at the Cu SC surface even when performing XPS sputter depth-profiling. Additionally, ion scattering spectroscopy (ISS) was performed on separate regions of these samples, but even this surface-sensitive technique did not indicate any glass contaminants on the surface.

Altogether, this suggests that the contaminants revealed by ICP can possibly influence the CV response by being present in the electrochemical double layer but without getting deposited on or incorporated into the Cu surface. Interestingly, a recent study by Bertheussen et al.[39] probing polycrystalline Cu (pc-Cu) under reaction conditions observed catalyst deactivation over time that was attributed to poisoning by deposited Si. They were actually able to detect Si on pc-Cu by XPS after performing CO reduction at −0.5 V vs RHE during prolonged EC measurements in a glass cell. To further investigate this aspect, we performed electrolyte exchange going from glass KOH to PFA KOH during EC measurements and observed the glass-induced features in the CV disappearing instantly (see Figure S4). Apparently in the case of SCs these contaminants are only loosely bound to the surface or present at the electrode/electrolyte interface.

So far, our data suggest negligible chemical modification of the surface during a typical EC measurement (duration: ∼1 hr), but the question still remains whether the surface was structurally altered during the EC measurement. In order to answer this, post-EC STM imaging was performed using the UHV-STM-EC setup. After the EC measurements, the samples were transferred back to UHV and STM was performed without any intermediate exposure to air. The sample analyzed was the Cu(111) exposed to KOH held overnight in the PFA flask. Figure 3 shows representative pre- and post-EC STM images. In both cases, the Cu(111) shows large terraces separated by monatomic steps. Furthermore, monatomic holes induced by the EC measurement are visible. However, no major structural changes like deep etch pits are visible, thus indicating that the overall surface structure remained intact during EC measurements, suggesting that the Cu(111) surface is relatively stable under these conditions.

We have shown how a combination of STM, EC, ICP-MS, and XPS can be used to investigate whether impurities are

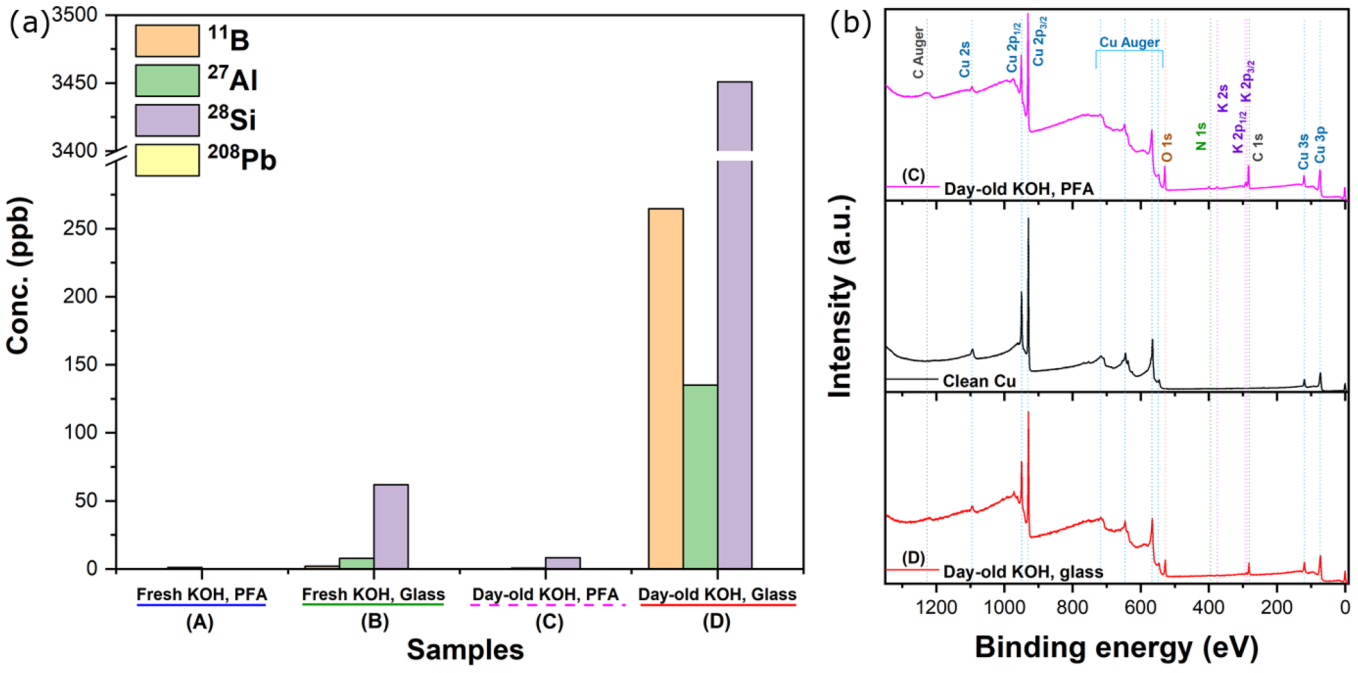

Figure 2. (a) ICP-MS measurements focusing on B, Al, Si, and Pb for the different electrolytes used. As can be seen, the KOH left overnight in a glass flask contains large amounts of contaminants compared to those from PFA flasks. (b) XPS surveys measured on the Cu(111) sample after the EC measurement and subsequent rinsing in deaerated Millipore water.

DOI: 10.1021/acsenergylett.9b01064
ACS Energy Lett. 2019, 4, 1645−1649

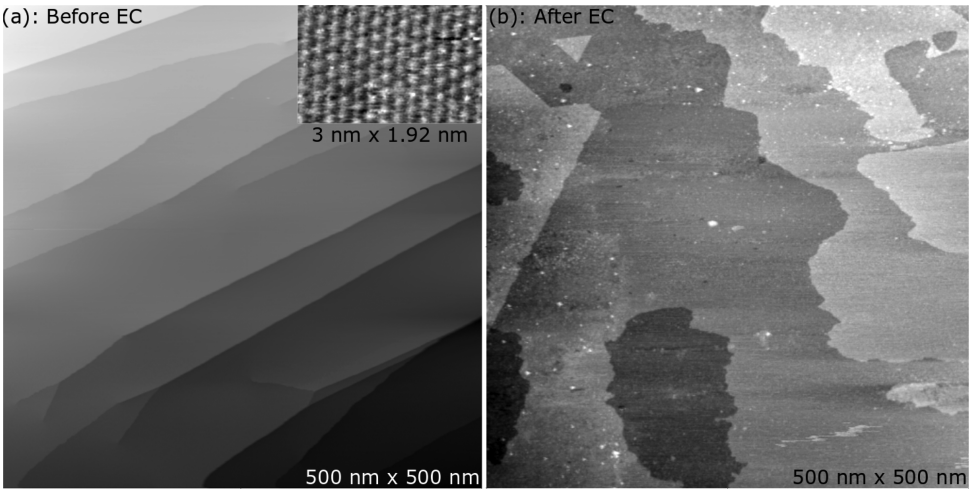

Figure 3. A comparison of the state of the Cu(111) surface before and after being cycled five times electrochemically between −0.2 and 0.45 V vs RHE in 0.1 M KOH as seen by STM. The inset in panel (a) shows atomic resolution of the surface.

affecting measurements adversely. In the present case it was shown that dissolved glassware in alkaline electrolyte completely changes the CV of Cu(111) from having one sharply peaked redox feature at 0.11 V vs RHE to having two anodic and two cathodic features. Furthermore, these features are separate from each other. Thus, we recommend avoiding all glassware in studies involving alkaline media as this can possibly affect the electrochemical behavior of a given system dramatically.

Aarti Tiwari
Thomas Maagaard
Ib Chorkendorff
Sebastian Horch*
Department of Physics, The Technical University of Denmark (DTU), Fysikvej 311, 2800 Kgs. Lyngby, Denmark

■ ASSOCIATED CONTENT

Supporting Information

The Supporting Information is available free of charge on the ACS Publications website at DOI: 10.1021/acsenergylett.9b01064.

Additional information on the experimental methods employed, including electrochemical results obtained on electropolished Cu(111) samples and a comparison to the literature (PDF)

■ AUTHOR INFORMATION

Corresponding Author

*E-mail: horch@fysik.dtu.dk.

ORCID

Aarti Tiwari: 0000-0002-8295-9420
Thomas Maagaard: 0000-0002-2306-1506
Ib Chorkendorff: 0000-0003-2738-0325
Sebastian Horch: 0000-0001-7601-9224

Notes

Views expressed in this Viewpoint are those of the authors and not necessarily the views of the ACS.
The authors declare no competing financial interest.

■ ACKNOWLEDGMENTS

This work was supported by Innovation Fund Denmark (IFD) under File No. 5160-00004B, research Grant 9455 from VILLUM FONDEN, and the European Union's Horizon 2020 research and innovation programme under the Marie Sklodowska-Curie Grant Agreement No. 713683.

■ REFERENCES

(1) Mistry, H.; Varela, A. S.; Kühl, S.; Strasser, P.; Cuenya, B. R. Nanostructured electrocatalysts with tunable activity and selectivity. *Nat. Rev. Mater.* **2016**, *1*, 16009.
(2) Stamenkovic, V. R.; Strmcnik, D.; Lopes, P. P.; Markovic, N. M. Energy and fuels from electrochemical interfaces. *Nat. Mater.* **2017**, *16*, 57−69.
(3) Seh, Z. W.; Kibsgaard, J.; Dickens, C. F.; Chorkendorff, I.; Nørskov, J. K.; Jaramillo, T. F. Combining theory and experiment in electrocatalysis: Insights into materials design. *Science* **2017**, *355*, eaad4998.
(4) Schouten, K. J. P.; Calle-Vallejo, F.; Koper, M. T. M. A Step Closer to the Electrochemical Production of Liquid Fuels. *Angew. Chem., Int. Ed.* **2014**, *53*, 10858−10860.
(5) Nielsen, D. U.; Hu, X.-M.; Daasbjerg, K.; Skrydstrup, T. Chemically and electrochemically catalysed conversion of CO2 to CO with follow-up utilization to value-added chemicals. *Nature Catalysis* **2018**, *1*, 244−254.
(6) Dinh, C.-T.; Burdyny, T.; Kibria, M. G.; Seifitokaldani, A.; Gabardo, C. M.; García de Arquer, F. P.; Kiani, A.; Edwards, J. P.; De Luna, P.; Bushuyev, O. S.; Zou, C.; Quintero-Bermudez, R.; Pang, Y.; Sinton, D.; Sargent, E. H. CO_2 electroreduction to ethylene via hydroxide-mediated copper catalysis at an abrupt interface. *Science* **2018**, *360*, 783−787.
(7) Bushuyev, O. S.; De Luna, P.; Dinh, C.-T.; Tao, L.; Saur, G.; van de Lagemaat, J.; Kelley, S. O.; Sargent, E. H. What Should We Make with CO_2 and How Can We Make It? *Joule* **2018**, *2*, 825.
(8) Gao, D.; Arán-Ais, R. M.; Jeon, H. S.; Roldan Cuenya, B. Rational catalyst and electrolyte design for CO2 electroreduction towards multicarbon products. *Nature Catalysis* **2019**, *2*, 198−210.
(9) Nitopi, S. A.; Bertheussen, E.; Scott, S. B.; Liu, X.; Engstfeld, A. K.; Horch, S.; Seger, B.; Stephens, I. E. L.; Chan, K.; Hahn, C.; Nørskov, J. K.; Jaramillo, T. F.; Chorkendorff, I. Progress and Perspectives of Electrochemical CO_2 Reduction on Copper in Aqueous Electrolyte. *Chem. Rev.* **2019**, DOI: 10.1021/acs.chemrev.8b00705.
(10) Hori, Y. In *Modern Aspects of Electrochemistry*; Vayenas, C., White, R., Gamboa-Aldeco, M., Eds.; Springer, 2008; Vol. 42; Chapter 3, pp 89−189.

DOI: 10.1021/acsenergylett.9b01064
ACS Energy Lett. 2019, 4, 1645−1649

(11) Li, C. W.; Kanan, M. W. CO_2 reduction at low overpotential on Cu electrodes resulting from the reduction of thick Cu2O films. *J. Am. Chem. Soc.* **2012**, *134*, 7231−7234.
(12) Frese, K. W., Jr. In *Electrochemical and Electrocatalytic Reactions of Carbon Dioxide*; Sullivan, B. P., Krist, K., Guard, H. E., Eds.; Elsevier: Amsterdam, 1993; Chapter 6, pp 145−216.
(13) Hori, Y.; Takahashi, I.; Koga, O.; Hoshi, N. Selective formation of C2 compounds from electrochemical reduction of CO2 at a series of copper single crystal electrodes. *J. Phys. Chem. B* **2002**, *106*, 15−17.
(14) Hori, Y.; Takahashi, I.; Koga, O.; Hoshi, N. Electrochemical reduction of carbon dioxide at various series of copper single crystal electrodes. *J. Mol. Catal. A: Chem.* **2003**, *199*, 39−47.
(15) Christophe, J.; Doneux, T.; Buess-Herman, C. Electroreduction of Carbon Dioxide on Copper-Based Electrodes: Activity of Copper Single Crystals and Copper-Gold Alloys. *Electrocatalysis* **2012**, *3*, 139−146.
(16) Schouten, K. J. P.; Qin, Z.; Pérez Gallent, E.; Koper, M. T. M. Two Pathways for the Formation of Ethylene in CO Reduction on Single-Crystal Copper Electrodes. *J. Am. Chem. Soc.* **2012**, *134*, 9864−9867.
(17) Schouten, K. J. P.; Pérez Gallent, E.; Koper, M. T. M. Structure Sensitivity of the Electrochemical Reduction of Carbon Monoxide on Copper Single Crystals. *ACS Catal.* **2013**, *3*, 1292−1295.
(18) Huang, Y.; Handoko, A. D.; Hirunsit, P.; Yeo, B. S. Electrochemical Reduction of CO2 Using Copper Single-Crystal Surfaces: Effects of CO* Coverage on the Selective Formation of Ethylene. *ACS Catal.* **2017**, *7*, 1749−1756.
(19) Le Duff, C. S.; Lawrence, M. J.; Rodriguez, P. Role of the Adsorbed Oxygen Species in the Selective Electrochemical Reduction of CO_2 to Alcohols and Carbonyls on Copper Electrodes. *Angew. Chem., Int. Ed.* **2017**, *56*, 12919−12924.
(20) Pérez-Gallent, E.; Marcandalli, G.; Figueiredo, M. C.; Calle-Vallejo, F.; Koper, M. T. M. Structure- and Potential-Dependent Cation Effects on CO Reduction at Copper Single-Crystal Electrodes. *J. Am. Chem. Soc.* **2017**, *139*, 16412−16419.
(21) Huang, Y.; Ong, C. W.; Yeo, B. S. Effects of Electrolyte Anions on the Reduction of Carbon Dioxide to Ethylene and Ethanol on Copper (100) and (111) Surfaces. *ChemSusChem* **2018**, *11*, 3299−3306.
(22) Lum, Y.; Ager, J. W. Evidence for product-specific active sites on oxide-derived Cu catalysts for electrochemical CO2 reduction. *Nature Catalysis* **2019**, *2*, 86−93.
(23) Engstfeld, A. K.; Maagaard, T.; Horch, S.; Chorkendorff, I.; Stephens, I. E. L. Polycrystalline and Single-Crystal Cu Electrodes: Influence of Experimental Conditions on the Electrochemical Properties in Alkaline Media. *Chem. - Eur. J.* **2018**, *24*, 17743−17755.
(24) Droog, J. M.; Schlenter, B. Oxygen electrosorption on copper single crystal electrodes in sodium hydroxide solution. *J. Electroanal. Chem. Interfacial Electrochem.* **1980**, *112*, 387−390.
(25) Jovic, V. D.; Jovic, B. M. Surface reconstruction during the adsorption/desorption of OH species onto Cu(111) and Cu(100) in 0.1 M NaOH solution. *J. Serb. Chem. Soc.* **2002**, *67*, 531−546.
(26) Jovic, V. D.; Jovic, B. M. EIS and differential capacitance measurements onto single crystal faces in different solutions Part II: Cu (111) and Cu (100) in 0.1 M NaOH. *J. Electroanal. Chem.* **2003**, *541*, 13−21.
(27) P. Schouten, K. J. P.; Gallent, E. P.; Koper, M. T. M. The electrochemical characterization of copper single-crystal electrodes in alkaline media. *J. Electroanal. Chem.* **2013**, *699*, 6−9.
(28) Härtinger, S.; Pettinger, B.; Doblhofer, K. Cathodic formation of a hydroxide adsorbate on Cu(111) electrodes in alkaline electrolyte. *J. Electroanal. Chem.* **1995**, *397*, 335−338.
(29) Maurice, V.; Strehblow, H.-H.; Marcus, P. In situ STM study of the initial stages of oxidation of Cu(111) in aqueous solution. *Surf. Sci.* **2000**, *458*, 185−194.
(30) Kunze, J.; Maurice, V.; Klein, L. H.; Strehblow, H.-H.; Marcus, P. In Situ Scanning Tunneling Microscopy Study of the Anodic Oxidation of Cu(111) in 0.1 M NaOH. *J. Phys. Chem. B* **2001**, *105*, 4263−4269.
(31) Rinaldo, S. G.; Lee, W.; Stumper, J.; Eikerling, M. Mechanistic Principles of Platinum Oxide Formation and Reduction. *Electrocatalysis* **2014**, *5*, 262−272.
(32) Kristoffersen, H. H.; Vegge, T.; Hansen, H. A. OH formation and H_2 adsorption at the liquid water-Pt(111) interface. *Chemical Science* **2018**, *9*, 6912−6921.
(33) Hahn, C.; Hatsukade, T.; Kim, Y.-G.; Vailionis, A.; Baricuatro, J. H.; Higgins, D. C.; Nitopi, S. A.; Soriaga, M. P.; Jaramillo, T. F. Engineering Cu surfaces for the electrocatalytic conversion of CO 2: Controlling selectivity toward oxygenates and hydrocarbons. *Proc. Natl. Acad. Sci. U. S. A.* **2017**, *114*, 5918−5923.
(34) Cao, L.; Raciti, D.; Li, C.; Livi, K. J. T.; Rottmann, P. F.; Hemker, K. J.; Mueller, T.; Wang, C. Mechanistic Insights for Low-Overpotential Electroreduction of CO 2 to CO on Copper Nanowires. *ACS Catal.* **2017**, *7*, 8578−8587.
(35) Raciti, D.; Wang, C. Recent Advances in CO_2 Reduction Electrocatalysis on Copper. *ACS Energy Letters* **2018**, *3*, 1545−1556.
(36) Kim, Y. G.; Baricuatro, J. H.; Javier, A.; Gregoire, J. M.; Soriaga, M. P. The evolution of the polycrystalline copper surface, first to Cu(111) and then to Cu(100), at a fixed CO2RR potential: A study by operando EC-STM. *Langmuir* **2014**, *30*, 15053−15056.
(37) Mayrhofer, K. J. J.; Wiberg, G. K. H.; Arenz, M. Impact of Glass Corrosion on the Electrocatalysis on Pt Electrodes in Alkaline Electrolyte. *J. Electrochem. Soc.* **2008**, *155*, P1.
(38) Mayrhofer, K. J. J.; Crampton, A. S.; Wiberg, G. K. H.; Arenz, M. Analysis of the Impact of Individual Glass Constituents on Electrocatalysis on Pt Electrodes in Alkaline Solution. *J. Electrochem. Soc.* **2008**, *155*, P78.
(39) Bertheussen, E.; Hogg, T. V.; Abghoui, Y.; Engstfeld, A. K.; Chorkendorff, I.; Stephens, I. E. L. Electroreduction of CO on Polycrystalline Copper at Low Overpotentials. *ACS Energy Letters* **2018**, *3*, 634−640.

DOI: 10.1021/acsenergylett.9b01064
ACS Energy Lett. 2019, 4, 1645−1649